

# Circularly Polarized Light-Induced Magnetization Reversal in Bi,Ga-Substituted Magnetic Garnet Films

R. Asatani, S. Suzuki, A. Hata, M. A. A. Masud, H. Sakaguchi, S. Isogami\* and T. Ishibashi

Depart. Mater. Sci. and Bioeng., Nagaoka University of Technology, 1603-1 Kamitomioka, Nagaoka, Niigata 940-2188, Japan

\* Research Center for Magnetic and Spintronic Materials, National Institute for Materials Science, 1-2-1 Sengen, Tsukuba, Ibaraki 305-0047, Japan

All-optical magnetization switching (AOS) in magneto-optical materials is promising phenomena for applications such as high-speed optical modulation technology, as it allows for magnetization reversal using only ultrashort laser pulses. We report on AOS induced by circularly polarized light in Bi,Ga-substituted magnetic garnet,  $\text{Bi}_{2.5}\text{R}_{0.5}\text{Fe}_4\text{GaO}_{12}$  (R = Eu, Nd and Y), thin films prepared by the metal-organic decomposition method, which possess both large Faraday effect and perpendicular magnetic anisotropy. The experiments for circularly polarized light-induced magnetization reversal were performed using laser pulses with a wavelength of 514 nm and a pulse width of 230 fs. Helicity-dependent ring-shaped magnetic domains were formed around demagnetized domains for all samples, when approximately 200 pulses were cumulatively irradiated onto a single spot on the samples.

**Keywords:** magnetic garnet, ferrimagnetic materials, perpendicular magnetization, magneto-optical effect, circularly polarized light-induced magnetization reversal

## 1. Introduction

The advent of femtosecond pulsed lasers enabled the investigation of magnetization dynamics on timescales below 1 ps<sup>1</sup>. Subsequently, the phenomenon of All-optical magnetization switching (AOS) was discovered in Gd-Fe-Co thin films, where the magnetization reverses solely by the irradiation of a single laser pulse<sup>2</sup>. AOS is classified into helicity-independent AOS (HI-AOS) and helicity-dependent AOS (HD-AOS). Switching that is achieved with a single pulse is termed deterministic (or single-shot), while that which requires multiple pulses is referred to as cumulative (or multi-shot).

To date, deterministic HI-AOS has been reported in Gd-Fe-Co thin films<sup>3</sup> and Co-substituted Yttrium Iron Garnet (Co:YIG)<sup>4</sup>. Additionally, cumulative HI-AOS has been reported in materials such as  $\text{NiCo}_2\text{O}_4$ <sup>5</sup>. HI-AOS is a thermally driven process that has been reported to arise from differences in the demagnetization times of the spin sublattices of antiparallel aligned magnetic moments<sup>6</sup>. Consequently, HI-AOS has been considered a phenomenon unique to ferrimagnetic materials.

In contrast, deterministic HD-AOS has only been reported in Gd-Fe-Co thin films to date<sup>2,3</sup>. Other ferrimagnetic materials<sup>7</sup> and ferromagnetic materials, such as Co/Pt multilayer films<sup>8</sup>, exhibited cumulative HD-AOS. The mechanism of HD-AOS was initially attributed to the inverse Faraday effect (IFE)<sup>9</sup>. However, subsequent studies suggested that the magnetic circular dichroism (MCD) effect during light absorption<sup>10,11</sup> in magnetic materials played a more dominant role.

Bi-substituted magnetic garnets examined in this study are ferrimagnetic materials that exhibit large magneto-optical (MO) effects. Given these features, it is highly plausible that HD-AOS could be observed in Bi-substituted magnetic garnets, which possess large MO effects. However, no AOS reports concerning Bi-substituted magnetic garnets have been published to date. Therefore, in this study, we investigated circularly polarized light-induced magnetization reversal using Bi- and Ga-substituted magnetic garnet films,  $\text{Bi}_{2.5}\text{R}_{0.5}\text{Fe}_4\text{GaO}_{12}$  ( $\text{Bi}_{2.5}\text{Ga}_1\text{RIG}$ ) where R is rare-earth element, which possess excellent MO properties and perpendicular magnetic anisotropy (PMA). In this paper, we report on circularly polarized light-induced magnetization reversal in  $\text{Bi}_{2.5}\text{Ga}_1\text{RIG}$  (R = Eu, Nd and Y) upon cumulative irradiation with laser pulses of varying polarization states.

## 2. Bi,Ga-substituted rare-earth iron garnet

Rare-earth iron garnets,  $\text{R}_3\text{Fe}_5\text{O}_{12}$  (RIG) have a garnet crystal structure, in which iron ions,  $\text{Fe}^{3+}$ , occupy the tetrahedral and octahedral lattice sites, and rare-earth ions,  $\text{R}^{3+}$ , occupy the dodecahedral sites<sup>12</sup>. Within the molecular formula unit RIG,  $\text{Fe}^{3+}$  occupies three tetrahedral sites and two octahedral sites. Due to the antiferromagnetic coupling between these sites, the net magnetic moment per molecule  $|3 \times 5 \mu_B - 2 \times 5 \mu_B| = 5 \mu_B$ <sup>12</sup>. On the other hand, the magnetic moments of the rare-earth ions vary depending on the specific rare-earth element.

It is well known that substituting  $\text{Bi}^{3+}$  for  $\text{R}^{3+}$  significantly enhances the MO effect<sup>12</sup>. Furthermore,  $\text{Ga}^{3+}$  substitution enables to reduce the saturation magnetization, since it has no magnetic moment and 90%

---

Corresponding author: T. Ishibashi (e-mail: t\_bashi@mst.nagaokaut.ac.jp).

of the substituting  $\text{Ga}^{3+}$  replaces  $\text{Fe}^{3+}$  in the tetrahedral sites, resulting in a reduction of the demagnetization field ( $4\pi Ms$ )<sup>13,14</sup>. In this study, Bi substitution amount was set to 2.5 to achieve a large Faraday rotation angle. In addition, to achieve PMA, the Ga substitution amount was set to 1.0 to decrease demagnetization field<sup>14</sup>, and  $\text{Gd}_3\text{Ga}_5\text{O}_{12}$  (GGG) single-crystal substrate with a (111) orientation was chosen to utilize that RIGs have the easy-axis of magnetization along the (111). Furthermore, to investigate the rare-earth ion dependence of the AOS induced by circularly polarized light, Eu, Nd and Y were selected as the rare-earth elements, where magnetic moments of  $\text{Eu}^{3+}$ ,  $\text{Nd}^{3+}$  and  $\text{Y}^{3+}$  are oriented antiparallel, parallel, and exhibit no moment, respectively, with respect to the net magnetic moment of  $\text{Fe}^{3+}$  in the garnet structure<sup>12-16</sup>.

$\text{Bi}_{2.5}\text{Ga}_1\text{:RIG}$  (R = Eu, Nd and Y), i.e.  $\text{Bi}_{2.5}\text{Ga}_1\text{:EIG}$ ,  $\text{Bi}_{2.5}\text{Ga}_1\text{:NIG}$  and  $\text{Bi}_{2.5}\text{Ga}_1\text{:YIG}$ , thin films were prepared on GGG (111) substrates using the MOD method<sup>12</sup>. The MOD solutions, produced by Kojundo Chemical Laboratory Co., Ltd. were used.  $\text{Bi}_{2.5}\text{Ga}_1\text{:EIG}$  thin film was prepared using MOD solution prepared by mixing the MOD solutions,  $\text{BiEuFe-04}(2.5/0.5/5)$  and  $\text{BiEuFeGa-04}(2.5/0.5/3/2)$ , in a 1:1 ratio.  $\text{Bi}_{2.5}\text{Ga}_1\text{:NIG}$  and  $\text{Bi}_{2.5}\text{Ga}_1\text{:YIG}$  thin films were prepared using  $\text{BiNdFeGa-04}(2.5/0.5/4/1)$  and  $\text{BiYFeGa-04}(2.5/0.5/4/1)$ , respectively. For the MOD method, the GGG (111) substrate was placed in a spin coater, coated with the MOD solution, and spun at 3000 rpm for 30 s. This was followed by a drying process on a hot plate at 100°C for 10 min, and then a pre-annealing at 450°C for 10 min. In this study, the coating to pre-annealing process was repeated five times, followed by a final annealing at 700°C for 3 h in an electric furnace. The total film thickness fabricated by this process is estimated to be approximately 150 nm.

The crystallinity of prepared  $\text{Bi}_{2.5}\text{Ga}_1\text{:RIG}$  thin films was characterized by the X-ray diffractometer (XRD) (Rigaku, SmartLab) using  $\text{CuK}\alpha_1$  radiation ( $\lambda = 0.154059$  nm) for out-of-plane measurements monochromized with a double Ge (220) monochromator. Faraday rotation and ellipticity spectra and Faraday rotation hysteresis were measured using MO spectrometer, and magnetic domain

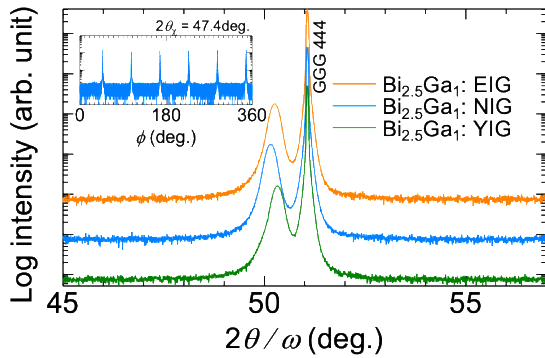


**Fig.1** X-ray diffraction patterns of  $\text{Bi}_{2.5}\text{Ga}_1\text{:EIG}$ ,  $\text{Bi}_{2.5}\text{Ga}_1\text{:NIG}$  and  $\text{Bi}_{2.5}\text{Ga}_1\text{:YIG}$  thin films.

structures were measured using MO imaging technique.

Figure 1 shows XRD patterns ( $2\theta/\omega$  scan) of  $\text{Bi}_{2.5}\text{Ga}_1\text{:EIG}$ ,  $\text{Bi}_{2.5}\text{Ga}_1\text{:NIG}$  and  $\text{Bi}_{2.5}\text{Ga}_1\text{:YIG}$  thin films, where an inset shows  $\phi$  scan for (422) of  $\text{Bi}_{2.5}\text{Ga}_1\text{:NIG}$ . Diffraction peaks were clearly observed in the lower angle side of GGG 444 peak for all samples, which can be estimated as 444 diffraction peaks of  $\text{Bi}_{2.5}\text{Ga}_1\text{:EIG}$ ,  $\text{Bi}_{2.5}\text{Ga}_1\text{:NIG}$  and  $\text{Bi}_{2.5}\text{Ga}_1\text{:YIG}$  thin films, respectively. The  $\phi$  scan of the  $\text{Bi}_{2.5}\text{Ga}_1\text{:NIG}$  showed 6-fold symmetry,

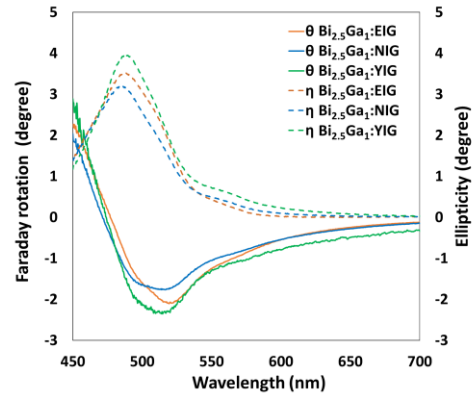


**Fig.2** Faraday rotation (solid line) and Ellipticity (dotted line) spectra of  $\text{Bi}_{2.5}\text{Ga}_1\text{:EIG}$ ,  $\text{Bi}_{2.5}\text{Ga}_1\text{:NIG}$  and  $\text{Bi}_{2.5}\text{Ga}_1\text{:YIG}$  thin films.

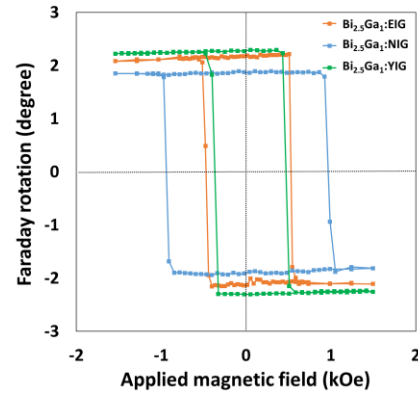


**Fig. 3** Faraday rotation hysteresis of  $\text{Bi}_{2.5}\text{Ga}_1\text{:EIG}$ ,  $\text{Bi}_{2.5}\text{Ga}_1\text{:NIG}$  and  $\text{Bi}_{2.5}\text{Ga}_1\text{:YIG}$  thin films.

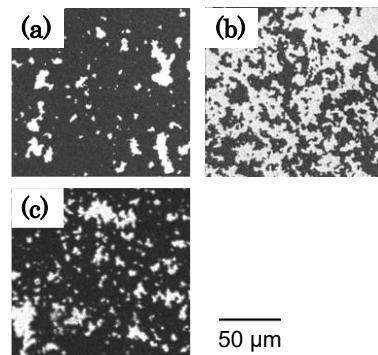


**Fig. 4** MO images measured for demagnetized states of (a)  $\text{Bi}_{2.5}\text{Ga}_1\text{:EIG}$ , (b)  $\text{Bi}_{2.5}\text{Ga}_1\text{:NIG}$  and (c)  $\text{Bi}_{2.5}\text{Ga}_1\text{:YIG}$  thin films.

and similar results were obtained for the other two samples, not shown here. These results suggested that all samples were epitaxially grown with (111) orientation on GGG substrates. The out-of-plane lattice constants for the Bi<sub>2.5</sub>Ga<sub>1</sub>:EIG, Bi<sub>2.5</sub>Ga<sub>1</sub>:NIG and Bi<sub>2.5</sub>Ga<sub>1</sub>:YIG thin films were obtained to be 1.258, 1.260 and 1.255 nm, respectively.

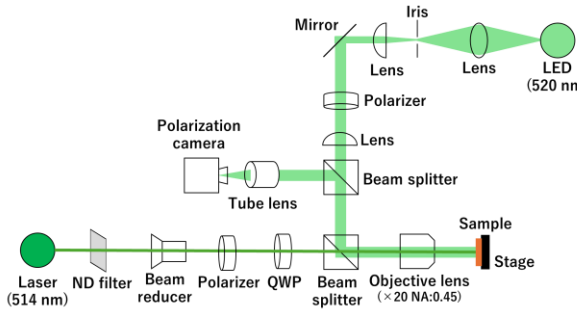
Figure 2 shows Faraday rotation and ellipticity spectra of all samples, exhibiting the characteristic spectral shape of Bi-substituted rare-earth iron garnets. Faraday rotation and ellipticity angles at a wavelength of 514 nm were approximately -2° and 2°, respectively. Figure 3 shows Faraday rotation hysteresis of Bi<sub>2.5</sub>Ga<sub>1</sub>:EIG (at  $\lambda = 519$  nm), Bi<sub>2.5</sub>Ga<sub>1</sub>:NIG (at  $\lambda = 514$  nm) and Bi<sub>2.5</sub>Ga<sub>1</sub>:YIG (at  $\lambda = 514$  nm) thin films. The magnetic hysteresis loops showed a square shape, although the coercivity field ( $H_c$ ) varied among the samples. These results suggested that the magnetic and MO characteristics in Bi<sub>2.5</sub>Ga<sub>1</sub>:RIG do not significantly depend on the rare-earth element.

Figure 4 shows MO images of Bi<sub>2.5</sub>Ga<sub>1</sub>:EIG, Bi<sub>2.5</sub>Ga<sub>1</sub>:NIG and Bi<sub>2.5</sub>Ga<sub>1</sub>:YIG measured at demagnetization states. Magnetic domain patterns indicating perpendicular magnetization are clearly observed. Many magnetic domains measuring several tens of microns were observed in the Bi<sub>2.5</sub>Ga<sub>1</sub>:EIG thin film, and it was found that their size was larger than that of Bi<sub>2.5</sub>Ga<sub>1</sub>:NIG or Bi<sub>2.5</sub>Ga<sub>1</sub>:YIG.

### 3. AOS experiments

Figure 5 illustrates the optical setup used in this experiment, which integrates the laser excitation and magneto-optical Kerr microscopy systems. The irradiation was performed using a Yb:KGW laser operating at a wavelength of 514 nm, a pulse duration of 230 fs, and a repetition rate of 10 kHz. A polarizer and a quarter-wave plate (QWP) were used to control the polarization state of the laser beam. The polarization-controlled laser pulses were focused onto the sample using a 20× objective lens with a numerical aperture (NA) of 0.45. The sample was fixed onto a sample stage capable of movement along the x and y axes. Observation of the formed magnetic domains was performed using a green LED with a wavelength of 520 nm as the light source and a polarization camera<sup>17)</sup>.

Laser pulses were delivered using both cumulative and

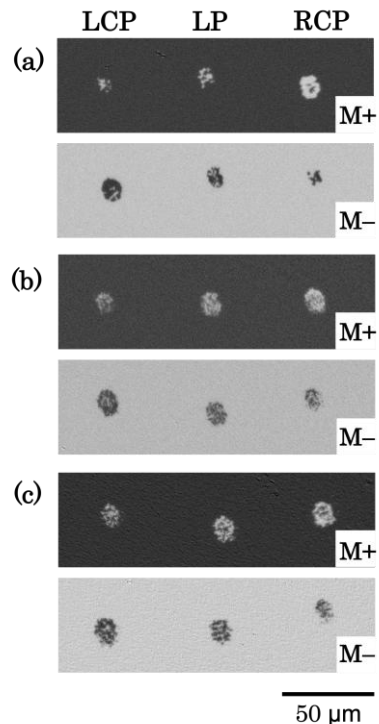


**Fig. 5** Optical setup for AOS experiments.

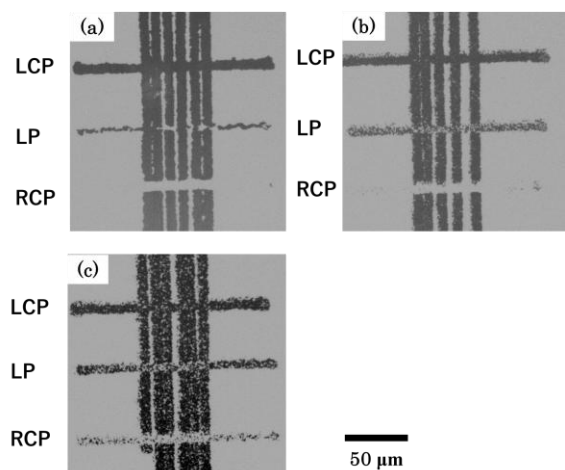
scanning irradiation methods. In cumulative irradiation, the number of pulses directed onto the same spot was controlled by a shutter. In scanning irradiation, the sample stage was moved at a constant speed of approximately 50  $\mu\text{m/s}$  during laser exposure. These experiments were conducted at room temperature (RT) and in ambient air. Prior to laser irradiation, an external magnetic field was applied to the sample to achieve magnetic saturation (i.e., aligning the magnetization uniformly in one direction).

Figure 6 shows the magnetic domain images of the Bi<sub>2.5</sub>Ga<sub>1</sub>:EIG, Bi<sub>2.5</sub>Ga<sub>1</sub>:NIG and Bi<sub>2.5</sub>Ga<sub>1</sub>:YIG film after cumulative irradiation with left-circularly polarized (LCP), linearly polarized (LP), and right-circularly polarized (RCP) light (from left to right) for both initial magnetization states, up (M+) and down (M-). The laser fluence for irradiation was set to 76  $\text{mJ/cm}^2$ , and the number of accumulated pulses was 200.

As shown in Fig.6(a), when the initial magnetization was upward, cumulative irradiation with LCP and LP resulted in a demagnetized state, characterized by magnetic domains randomly oriented both upward and downward. Cumulative irradiation with RCP revealed the formation of an annular magnetization reversal domain (AOS ring), which is characteristic of cumulative HD-AOS, with a demagnetized state inside the ring. Conversely, when the initial magnetization was downward, LCP irradiation resulted in the formation of AOS ring with a central demagnetized state, while LP



**Fig. 6** MO images of (a) Bi<sub>2.5</sub>Ga<sub>1</sub>:EIG, (b) Bi<sub>2.5</sub>Ga<sub>1</sub>:NIG and (c) Bi<sub>2.5</sub>Ga<sub>1</sub>:YIG thin films. Initial magnetization direction: Black represents upward (M+), and white represents downward (M-).



**Fig. 7** MO images of (a)  $\text{Bi}_{2.5}\text{Ga}_1\text{:EIG}$ , (b)  $\text{Bi}_{2.5}\text{Ga}_1\text{:NIG}$  and (c)  $\text{Bi}_{2.5}\text{Ga}_1\text{:YIG}$  thin films measured after scanning irradiation with LCP, LP and RCP, where vertical line-shaped magnetic domains with opposite magnetization state  $M^+$  were written in advance by the scanning irradiation with LCP.

and RCP resulted only in a demagnetized state. Cumulative irradiation experiments were also conducted on  $\text{Bi}_{2.5}\text{Ga}_1\text{:NIG}$  and  $\text{Bi}_{2.5}\text{Ga}_1\text{:YIG}$  as shown in Figs. 6(b) and 6(c), respectively. In both samples, helicity-dependent AOS rings formed during the cumulative irradiation process as observed for the  $\text{Bi}_{2.5}\text{Ga}_1\text{:EIG}$  thin film.

Figure 7 shows MO images of the  $\text{Bi}_{2.5}\text{Ga}_1\text{:EIG}$ ,  $\text{Bi}_{2.5}\text{Ga}_1\text{:NIG}$  and  $\text{Bi}_{2.5}\text{Ga}_1\text{:YIG}$  films measured after the scanning irradiation with LCP, LP and RCP with a laser fluence of  $58 \text{ mJ/cm}^2$ . Before the scanning with the three polarization states, the samples were magnetized in a downward magnetization state  $M^-$ , and 5 or 6 vertical line-shaped magnetic domains with opposite magnetization state  $M^+$  were written by the scanning irradiation with LCP light at the same power. As shown in Fig. 7, regardless of the type of rare earth element in the samples, line-shaped magnetic domains with  $M^+$  and  $M^-$  were obtained for LCP and RCP, respectively, and demagnetized domains were obtained for LP. These results clearly demonstrate HD-AOS in Bi-substituted rare-earth iron garnets, which is consistent with the results of other studies on HD-AOS<sup>2,3,5,7,8</sup>. The details of the rare earth dependence of HD-AOS will be reported in the near future.

Focusing on the MCD effect, which is considered crucial for the manifestation of HD-AOS, the  $\text{Bi}_{2.5}\text{Ga}_1\text{:RIG}$  film exhibits a large ellipticity angle. The ellipticity angle remains nearly constant even when the rare-earth ion is altered. Consequently, it is suggested that HD-AOS manifested similarly across the three  $\text{Bi}_{2.5}\text{Ga}_1\text{:RIG}$  samples. In other words, this high MCD effect is considered to play a major role in the manifestation of HD-AOS in Bi-substituted rare-earth

iron garnets.

#### 4. Conclusion

In conclusion, we demonstrated that the magnetization of  $\text{Bi}_{2.5}\text{Ga}_1\text{:EIG}$ ,  $\text{Bi}_{2.5}\text{Ga}_1\text{:NIG}$  and  $\text{Bi}_{2.5}\text{Ga}_1\text{:YIG}$  thin films can be reversed by circularly polarized laser pulses without an external magnetic field, using a pulsed laser operating at a wavelength of 514 nm, a pulse duration of 230 fs, and a repetition rate of 10 kHz. This magnetization reversal is determined by the helicity of the circularly polarized light. We considered that high MCD effect of Bi,Ga-substituted magnetic garnets plays a major role in the manifestation of HD-AOS.

**Acknowledgements** This work was supported by NIMS Joint Research Hub Program.

#### References

- 1) E. Beaurepaire, J.-C. Merle, A. Daunois, and J.-Y. Bigot: *Phys. Rev. Lett.*, **76**, 4250(1996)
- 2) C. D. Stanciu, F. Hansteen, A. V. Kimel, A. Kirilyuk, A. Tsukamoto, A. Itoh and Th. Rasing: *Phys. Rev. Lett.*, **99**, 047601 (2007)
- 3) T. Ohkochi, R. Takahashi, H. Fujiwara, H. Takahashi, R. Adam, U. Parlak, K. Yamamoto, H. Osawa, M. Kotsugi, A. Tsukamoto, H. Wadati, A. Sekiyama, C. M. Schneider, M. Tsunoda, S. Suga and T. Kinoshita: *J. Magn. Magn. Mat.*, **593**, 171854 (2024)
- 4) A. Stupakiewicz, K. Szerenos, D. Afanasiev, A. Kirilyuk, and A.V. Kimel: *Nature*, **542**, 71(2017)
- 5) R. Takahashi, T. Ohkochi, D. Kan, Y. Shimakawa and H. Wadati: *ACS Appl. Electron. Mater.*, **5**, 748(2023)
- 6) I. Radu, K. Vahaplar, C. Stamm, T. Kachel, N. Pontius, H. A. Dürr, T. A. Ostler, J. Barker, R. F. L. Evans, R.W. Chantrell, A. Tsukamoto, A. Itoh, A. Kirilyuk, Th. Rasing and A. V. Kimel: *Nature*, **472**, 205(2011)
- 7) A. Ciuciulkaite, K. Mishra, M. V. Moro, I.-A. Chioar, R. M. R. Robinson, S. Parchenko, A. Kleibert, B. Lindgren, G. Andersson, C. S. Davies, A. Kimel, M. Berritta, P. M. Oppeneer, A. Kirilyuk and V. Kapaklis: *Physical Review Materials*, **4**, 104418 (2020)
- 8) U. Parlak, R. Adam, D. E. Bürgler, S. Gang, and C. M. Schneider: *Phys. Rev. B*, **98**, 214443 (2018)
- 9) T.D. Cornelissen, R. Cordoba and B. Koopmans: *Appl. Phys. Lett.*, **108**, 142405(2016)
- 10) A.R. Khorsand, M. Savoini, A. Kirilyuk, A.V. Kimel, A. Tsukamoto, A. Itoh and Th. Rasing: *Phys. Rev. Lett.*, **108**, 127205(2012)
- 11) J. Gorchon, Y. Yang and J. Bokor: *Phys. Rev. B*, **94**, 020409(R) (2016)
- 12) T. Ishibashi: *J. Magn. Soc. Jpn.*, **44**, 108(2020)
- 13) G. Lou, T. Kato, S. Iwata and T. Ishibashi: *Optical Materials Express*, **7**, 2248(2017)
- 14) M. Sasaki, G. Lou, Q. Liu, M. Ninomiya, T. Kato, S. Iwata and T. Ishibashi: *J. Appl. Phys.*, **55**, 055501(2016)
- 15) M. A. A. Masud, W. Asano, K. Watanabe, M. Kawahara, F. Z. Chafi, M. Nishikawa, and T. Ishibashi, *IEEE Trans. Magn.*, **61**, 1 (2025)
- 16) R. Pauthenet: *J. Appl. Phys.*, **29**, 253 (1958)
- 17) H. Sakaguchi, R. Oya, S. Wada, T. Matsumura, H. Saito and T. Ishibashi: *J. Magn. Soc. Jpn.*, **46**, 37(2022)

**Received Oct. 26, 2025; Accepted Jan. 6, 2026**